ELSEVIER

Polymer 44 (2003) 2169–2176

polymer

www.elsevier.com/locate/polymer

Computational studies of the Brookhart's type catalysts for ethylene polymerisation. Part 2: ethylene insertion and chain transfer mechanisms

J. Ramos[a], V. Cruz[b], A. Muñoz-Escalona[a], S. Martínez[a], J. Martínez-Salazar[a,*]

[a]*Instituto de Estructura de la Materia, GIDEM, C.S.I.C, Serrano 113bis, 28006 Madrid, Spain*
[b]*Centro Técnico de Informatica, C.S.I.C, Pinar 19, 28006 Madrid, Spain*

Received 7 November 2002; received in revised form 29 January 2003; accepted 29 January 2003

Abstract

This report describes complete density functional theory studies performed to elucidate ethylene polymerisation mechanisms of the Brookhart-type catalysts *N*,*N*′-(2,6-dimethylphenyl)ethylenediimine nickel (II) and *N*-(2,6-dimethylphenyl)pyridine-2-carboxaldiimine nickel (II). Both catalysts showed conformations that blocked the active site and thus hindered ethylene coordination. These conformations were related to the rotational capacity of the ancillary aryl group attached to the ligands, which generates agostic interactions between nickel and hydrogen atoms. It was calculated that these conformations were 8.3 and 10.7 kcal/mol (respectively for each catalyst) more stable than non-blocking cationic conformations. From a design perspective, catalytic systems would need to include bulky constituents to avoid these types of blocking conformation. The two possible mechanisms already proposed for the chain initiation step evoke approaches for ethylene inside and out of the equatorial plane of the catalyst. Herein, the in-plane mechanism was found to be the most favourable. However, for chain propagation, the out-plane approach for ethylene proved to be the most feasible, due to nickel agostic interactions with the growing alkyl chain. The energy barriers calculated for the propagation step were 9.3 and 10.6 kcal/mol for the two catalysts, respectively. These findings indicate the ethylenediimine catalyst is slightly more active than the pyridine catalyst. Three possible chain transfer mechanisms were also considered for the two catalysts: β-hydride transfer, β-hydride transfer to monomer and an association mechanism; the last two being the mostly likely mechanisms in thermodynamics and kinetic terms. Chain transfer processes for the pyridine-2-carboxaldiimine based catalyst were found to be more favourable than those of the ethylenediimine based catalyst. This finding is in agreement with experimental results which indicate that the former catalyst gives rise to lower molecular weight polymers.

Keywords: DFT; Brookhart catalyst; Ethylene polymerisation

1. Introduction

Since the 1980s, the use of organometallic compounds as single site catalysts in polymer production has been the subject of intense research. In particular, group 4 metallocene complexes have been both experimentally [1–3] and theoretically [4–11] described as chemically well-defined and highly active catalysts for homogeneous olefin polymerisation. There is current growing interest, however, in developing alternative organometallic compounds aimed at providing catalyst systems that are easier to elaborate, thus avoiding undesirable litigation related to patents. Over the last few years, Ni(II) bulk diimine complexes synthesized by Brookhart's group [12–14] and Fe(II) bisiminopyridine complexes independently generated by the groups of Gibson and Brookhart [15–18] have emerged as alternative catalytic systems for olefin polymerisation.

It is well known that organometallic compounds based on group 10 transition metals (mainly nickel and palladium) can only give rise to ethylene oligomers. This suggests an easy chain transfer process relative to the insertion step [19]. However, in 1995, Brookhart's group reported the production of high molecular weight polyethylene using nickel bulk α-diimine complexes. Based on this seminal work, recent efforts have centred on the use of non-metallocene compounds as catalysts for ethylene polymerisation [12–14]. This renewed interest prompted an exhaustive review by Brookhart et al. [20], which considers a plethora of nickel diimine complexes as potential catalysts for ethylene polymerisation. From these, we selected nickel

* Corresponding author. Tel: +34-915901618; fax: +34-915855413.
E-mail address: jmsalazar@iem.cfmac.csic.es (J. Martínez-Salazar).

0032-3861/03/$ - see front matter © 2003 Elsevier Science Ltd. All rights reserved.
doi:10.1016/S0032-3861(03)00088-0

complexes based on the α-diimine ligands, ethylenediimine (or Brookhart catalyst) and pyridine-2-carboxaldiimine (herein denoted pyridine catalyst), as representative structures for this type of catalyst [21–23]. The structure of these catalysts can be generally described as a square-plane environment around the nickel atom. The methyl groups or halogen atoms bonded to the nickel atom and the α-diimine ligand take up the coordination sites that belong to the square-plane. The aryl groups attached to the N atom of the α-diimine ligand remain perpendicular to the molecular plane of the complex, overcrowding its axial positions.

The following are the most significant experimental features reported for Brookhart catalysts [12–14]: (i) they are the first group 10 complexes known to polymerise α-olefins, in some cases yielding living polymerisation systems; (ii) the resting state of the ethylene π-complex between consecutive insertions has been observed using experimental techniques (NMR) [12]; and (iii) reducing the steric bulk of the α-diimine ligand leads to a decrease in polymer molecular weight [12].

Due to the complexity of the catalytic system, several approaches to the theoretical analysis of Brookhart catalysts in ethylene polymerisation have been described. These include building a simpler catalyst model than the real catalytic system [24–26] or partitioning the real system using integrated QM/MM methods [27–28]. In the present study, however, we considered a system in which all atoms are treated at the level of density functional theory (DFT).

In the first section, we report theoretical results related to the effects of active site conformations on the catalytic activity of two different Brookhart catalysts using DFT models. Our aim was to extend present knowledge by exploring ethylene insertion and chain transfer mechanisms for the two nickel-based imine catalysts, *N*,*N*′-(2,6-dimethylphenyl)ethylenediimine nickel (II) (hereafter denoted Brookhart catalyst) and *N*-(2,6-dimethylphenyl)-pyridine-2-carboxaldiimine nickel (II) (hereafter denoted pyridine catalyst) [29,30]. It is worthwhile to explore how substituting an aryl group attached to the diimine ligand with a pyridine group affects the performance of these catalysts would have applications in the design of this type of system.

2. Computational methods

Geometries and energies were obtained by the BP86 method implemented in the Amsterdam Density Functional (ADF) package [31]. This method comprises local density approximations according to Vosko et al. [32], adding non-local corrections to exchange according to Perdew [33] and correlation according to Becke [34]. Innermost atomic shells for all atoms were treated within the frozen core approximation to minimise computational effort. Outermost shells were described using/according to a triple-ζ basis set plus a polarisation function on the nickel atom. A double-ζ basis set, augmented with a polarisation function, was used for the remaining atoms. The approximate reaction paths were evaluated by a linear synchronous transit (LST) calculation. The reaction coordinate was taken as the distance between the midpoint of the ethylene monomer and the Ni atom.

3. Results and discussion

First of all, the differences between Brookhart **1a** and pyridine **2a** catalysts should be clarified (see Scheme 1). Due to the presence of the pyridine group, pyridine **2a** complexes are not symmetrical with respect to the axial plane. As a consequence, pyridine catalysts contain two non-equivalent sites for ethylene coordination and subsequent insertions into the metal–carbon bond (site **A** and **B**, Scheme 1). In contrast, in the Brookhart **1a** catalyst, the two possible vacant sites are equivalent. The **A** and **B** sites of the pyridine catalyst are not independent because of the migratory insertion mechanism of the polymerisation reaction, which makes the growing polymer chain alternate from one site to another. Therefore, ethylene coordination and insertion at both **A** and **B** sites have to be considered for the pyridine catalyst.

In the subsections below, the ethylene polymerisation process catalysed by the Brookhart **1a** and pyridine **2a** catalytic systems will be discussed according to the following steps: (i) conformations of the cationic methyl active species followed by ethylene coordination, (ii) chain initiation, (iii) chain propagation and (iv) possible chain transfer reactions. In the last subsection, we will compare propagation and chain transfer mechanisms.

3.1. Conformations of the cationic methyl active species followed by monomer coordination

The cationic methyl conformers of the Brookhart **1a** catalyst have been reported in our previous paper [35]. We will therefore only mention the most relevant features to be compared with the pyridine **2a** catalyst. Fig. 1, Table 1 and Fig. 2, Table 2 show conformations and relative energies for the Brookhart **1a** and pyridine **2a** catalysts, respectively.

Four stationary points corresponding to the most stable conformations of the cationic alkyl active species were

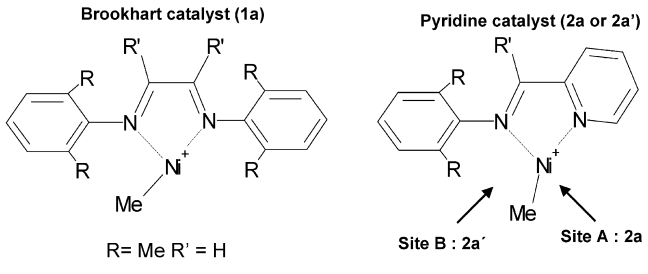

Scheme 1.

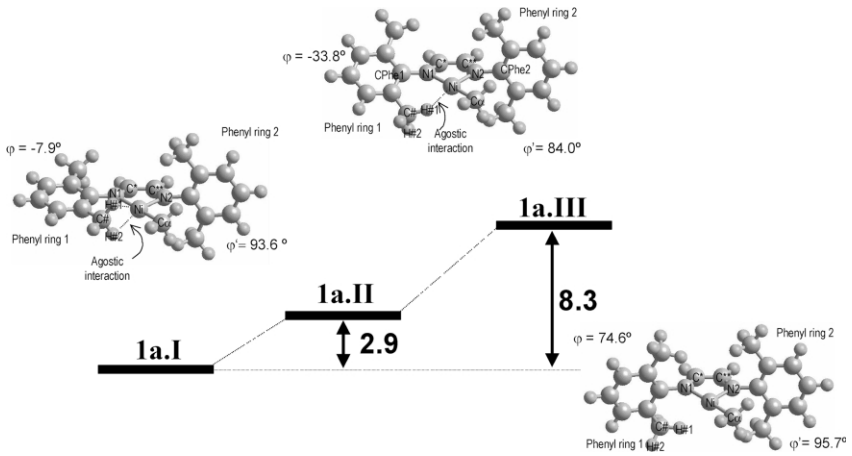

Fig. 1. Relative energies for the cationic active site conformers of the Brookhart **1a** catalyst given in kcal/mol.

observed in the pyridine **2a** catalyst. The main geometrical difference between them can be represented by the φ angle. The value of the φ angle describes the position of aryl groups with respect to the plane formed by the pyridine-2-carboxaldiimine ligand and the nickel atom ($\varphi = 0°$ is an indication of a coplanar conformation). As opposed to the Brookhart **1a** catalyst, the pyridine **2a** catalyst presents two different perpendicular conformers depending on the position of the vacant site (**2a**.**III** for site **A** and **2a**.**IV** for site **B**). The most stable conformation found was the **2a**.**I** conformer, which has an almost coplanar aryl group ($\varphi = 0.1°$, see Fig. 2 and Table 2). This conformation is more stable than the perpendicular conformations **2a**.**IV** and **2a**.**III** ($\varphi = 88.5°$ and $\varphi = 90.6°$, respectively), with a difference of 8.3 and 10.7 kcal/mol. The geometrical arrangement of the **2a**.**I** conformation allows strong agostic interactions between the nickel atom and the hydrogen atoms of the methyl group attached to the aryl group (Ni–H#1 and Ni–H#2 distances are 1.890 and 1.886 Å, respectively, see Table 2). As a consequence, in the **2a**.**I** conformation, the vacant site is blocked, thus hindering ethylene coordination. This might result in an eventual decrease in catalyst activity, as has been described for the Brookhart **1a** catalyst [35]. Further, it was observed that the electronic energy barrier associated with ethylene coordination to **2a**.**III** or **2a**.**IV** is very low. In contrast, an electronic energy barrier of around 17.3 kcal/mol was estimated for conformation **2a**.**I**. These calculations were performed by LST using the mid ethylene–nickel atom distance as the reaction coordinate.

For both catalyst systems, the most stable conformation is the agostic coplanar one (**1a**.**I** and **2a**.**I**, Figs. 1 and 2), which is 8.3 and 10.7 kcal/mol lower in energy compared to the perpendicular conformations (**1a**.**III** and **2a**.**III**). In both

Table 1
Selected geometry parameters for cationic active site conformers of the Brookhart **1a** catalyst

Geometry parameters	Conformation		
	1a.**I**	**1a**.**II**	**1a**.**III**
Ni–Cα	1.944	1.936	1.913
Ni–H#1	**1.911**	**1.891**	2.773
Ni–H#2	**1.939**	2.575	4.194
C#–H#1	1.127	1.129	1.094
C#–H#2	1.123	1.099	1.093
Ni–N1	2.012	2.001	2.000
Ni–N2	1.895	1.885	1.862
N1–C*	1.308	1.308	1.303
N2–C* *	1.306	1.310	1.309
C*–C* *	1.442	1.437	1.440
N1–Cphe1	1.399	1.393	1.410
N2–Cphe2	1.431	1.429	1.428
CPhe1–N1–Ni	120.6	121.3	124.1
CPhe2–N2–Ni	128.3	128.1	125.2
N2–Ni–Cα	95.2	95.8	100.2
φ	−7.9	−33.8	74.6
φ'	93.6	84.0	95.7

Distances and angles are given in angstroms and degrees, respectively. Agostic interactions shown in bold.

Table 2
Selected geometric parameters for cationic active site conformers of the pyridine **2a** catalyst

Geometric parameters	Conformation			
	2a.**I**	**2a**.**II**	**2a**.**III**	**2a**.**IV**
Ni–Cα	1.951	1.951	1.911	1.900
Ni–H#1	**1.890**	2.090	3.660	4.755
Ni–H#2	**1.886**	**1.788**	3.807	3.148
C#–H#1	1.128	1.116	1.096	1.102
C#–H#2	1.129	1.140	1.103	1.097
Ni–N1	1.993	1.984	1.967	1.863
Ni–N2	1.905	1.915	1.880	2.040
N1–C*	1.301	1.299	1.289	1.301
N2–C* *	1.373	1.373	1.374	1.361
C*–C* *	1.449	1.447	1.452	1.446
N1–CPhe1	1.407	1.401	1.427	1.434
Cphe1–N1–Ni	119.3	119.7	125.7	125.8
N2–Ni–Cα	94.8	94.9	125.7	125.8
φ	0.1	15.8	90.6	88.5

Distances and angles are given in angstroms and degrees, respectively. Agostic interactions shown in bold.

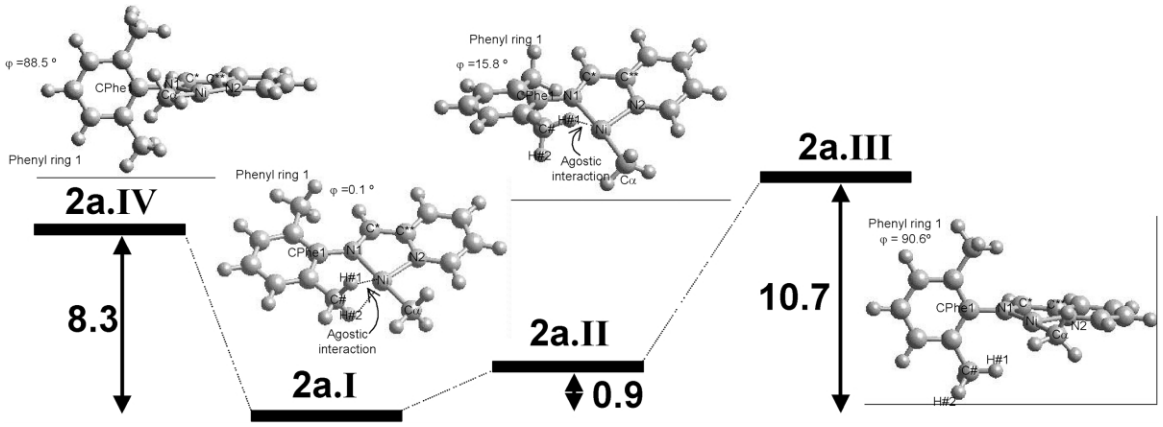

Fig. 2. Relative energies for the cationic active site conformers of the pyridine **2a** catalyst given in kcal/mol.

cases, agostic coplanar conformations block the vacant site for ethylene monomer coordination. LST calculations yielded energy barriers of 17.6 kcal/mol for **1a** and 17.3 kcal/mol for **2a**. Hence, the lower activity of both catalysts might be expected relative to that of systems with bulky constituents attached to the imine ligand, in which agostic coplanar conformations are impaired (Figs. 1 and 2) [35]. These theoretical results are in a good agreement with experimental observations (i.e. R = *i*Pr and R′ = Me or R = Me and R′ = Me) [12].

3.2. Chain initiation step

After the active site has formed, the polymer chain grows by starting with the first ethylene insertion step. Deng et al. [26] propose two mechanisms for this step: coordination of the incoming monomer in (in-plane path/pathway) or out of (out-plane path) the equatorial plane of the catalyst.

Energy profiles for the first ethylene insertion into the Brookhart (**1a**) and pyridine (**2a**, **2a′**) catalysts are represented in Fig. 3, while the corresponding energy values are given in Table 3. Ethylene coordination for the in-plane mechanism was always more favourable than the out-plane one (1.4, 3.2 and 3.7 kcal/mol for the **1a**, **2a** and **2a′** systems, respectively). This suggests that ethylene in-plane insertion is the preferred chain initiation step. Moreover, energy barriers for in-plane ethylene insertion were 10.5, 11.1 and 9.1 kcal/mol for the **1a**, **2a**, **2a′** systems, respectively (see $\Delta E_3^{\#}$ column in Table 3). Conversely, barriers for the out-plane ethylene insertion were 12.2, 12.0 and 10.7 kcal/mol for the **1a**, **2a**, **2a′** systems, respectively (see values in parenthesis in the $\Delta E_8^{\#}$ column in Table 3). It is clear that for both/all systems, energy barriers associated with the out-plane ethylene insertion mechanism are higher than those related to the in-plane insertion pathway (1.7, 0.9 and 1.6 kcal/mol for **1a**, **2a**, **2a′** systems, respectively).

In conclusion, ethylene coordination energies and insertion barriers point to the in-plane mechanism as the most favourable compared to the out-plane mechanism for both catalysts. The energy barriers for the first ethylene insertion in the pyridine **2a** catalyst were taken as the average of those for the **2a** and **2a′** systems, giving a value of 10.1 kcal/mol for the in-plane pathway and 11.3 kcal/mol for the out-plane approach. These averages are slightly lower that the energy barriers corresponding to the Brookhart **1a** catalyst. Furthermore, similar stabilities of

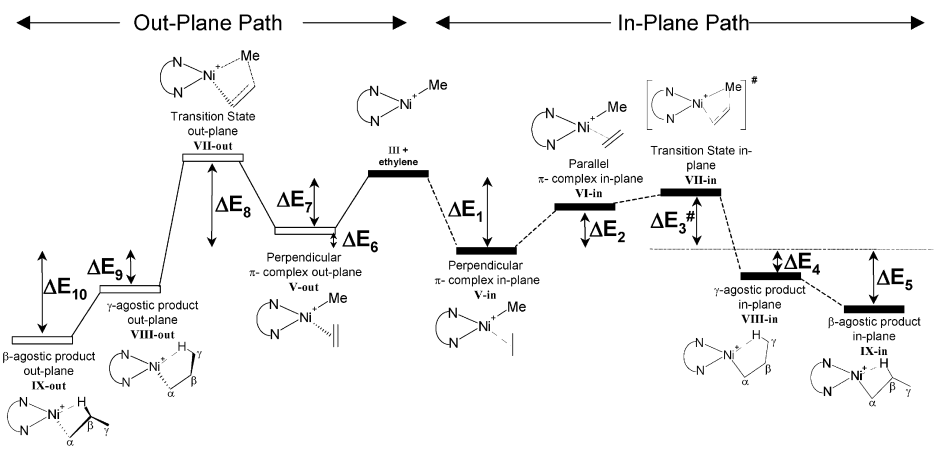

Fig. 3. Chain initiation step mechanism corresponding to the first ethylene insertion into the imine-nickel **1a**, **2a** and **2a′** systems, for in-plane and out-plane insertion paths/pathways. Energies were calculated relative to that of the in-plane perpendicular π-complex **V**-in (values provided in Table 3).

Table 3
Relative energies of the chain initiation step corresponding to the first ethylene insertion into the imine-nickel(II) **1a**, **2a** and **2a′** systems

System	In-plane path						Out-plane path			
	ΔE_1	ΔE_2	$\Delta E_3^{\#}$	ΔE_4	ΔE_5	ΔE_6	ΔE_7	$\Delta E_8^{\#}$	ΔE_9	ΔE_{10}
Brookhart **1a**	−28.5	8.0	10.5	−1.9	−9.9	1.4	−27.1	13.6 (12.2)	−0.7	−9.0
Pyridine **2a**	−32.5	9.3	11.1	−0.8	−9.6	3.2	−29.3	15.2 (12.0)	1.4	−8.5
Pyridine **2a′**	−32.2	8.9	9.1	−3.0	−9.6	3.7	−28.5	14.4 (10.7)	−1.1	−9.7

These energies are expressed in relation to that of the perpendicular in-plane π-complex **V**-in while those shown in parentheses are expressed in relation to that of the perpendicular out-plane π-complex **V-out.** (Energies given in kcal/mol).

the β-agostic product were noted after ethylene insertion in (**IX**-in) and out (**IX**-out) of plane. The calculations below for the chain propagation step were performed on the β-agostic insertion product in-plane (**IX**-in) as the resting state, since it is slightly more stable (see Fig. 4).

3.3. Chain propagation step

As in the chain initiation step, the incoming ethylene can approach the active site either in or out of plane. The ethylene out-plane approach is more stable by about 4–5 kcal/mol than the in-plane approach. This situation changes when compared to the first ethylene coordination.

Coordination energies for the chain propagation step were −14.5, −12.4 and −10.1 kcal/mol for the **1a**, **2a** and **2a′** systems, respectively (see Fig. 4 and Table 4). These values are considerably lower than those corresponding to the chain initiation step (compare ΔE_1 and ΔE_7 in Table 3 with ΔE_{11} in Table 4). Thus, ethylene coordination in the chain propagation step is less stable than in the chain initiation step. The β-agostic interaction presented in **IX**-in could be responsible for the energy drop in ethylene coordination, as the metal atom is electronically less demanding.

Energy barriers for the ethylene propagation step were 9.3, 11.1 and 10.1 for the **1a**, **2a** and **2a′** systems, respectively (see Fig. 4 and Table 4). As can be observed,

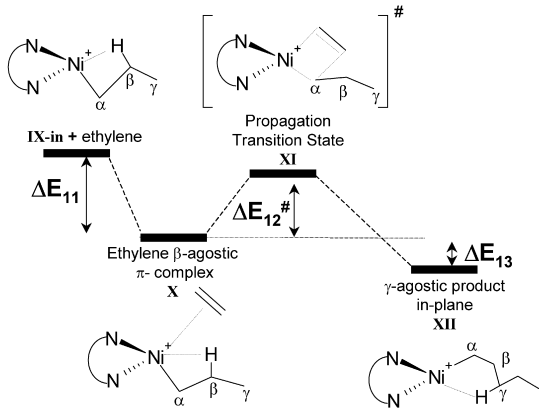

Fig. 4. Chain propagation step mechanism for ethylene polymerisation into the imine-nickel **1a**, **2a** and **2a′** systems. Energies were calculated relative to that of the ethylene propyl β-agostic π-complex (**X**) (values provided in Table 4).

the ethylene barrier propagation for the Brookhart **1a** catalyst (9.3 kcal/mol) is lower than the average energy barrier for the pyridine **2a** system (10.6 kcal/mol). This indicates that the Brookhart **1a** catalyst is slightly more active than the pyridine **2a** catalyst. This finding may help to clarify the contradictory results published in the patents and scientific literature regarding the catalytic activity of these complexes [21–23]. In each case, the direct insertion product shows a γ-agostic interaction (**XII**) which is more stable that the π-complex reactant (**X**). Chain growth continues by rotation of the alkyl chain produced by γ-agostic interaction finally giving rise to the β-agostic resting state.

3.4. Chain transfer processes

3.4.1. The β-hydride transfer mechanism

Fig. 5 and Table 5 show the energy profiles for the β-hydride transfer mechanism. The energy barriers ($\Delta E_{14}^{\#}$) associated with β-hydrogen transfer from the β-agostic conformer (**IX**) to the hydride vinyl π-complex (**XIV**) were 13.6, 11.5 and 10.2 kcal/mol for the **1a**, **2a** and **2a′** systems, respectively. In the hydride vinyl π-complex (**XIV**), the vinyl group can be either plane-in (**XIV**-in) or plane-out (**XIV**-out). For both catalysts the in-plane complex is the most stable system, energy barriers being 2.5, 0.5 and 2.3 kcal/mol for the **1a**, **2a** and **2a′** systems, respectively. The hydride vinyl π-complexes (**XIV**) develop into hydride complexes (**XV**) by ejection of the vinyl chain. These complexes (**XV**) are more unstable by 48.2, 47.6 and 47.7 kcal/mol for the **1a**, **2a** and **2a′** systems, respectively (see ΔE_{17} in Table 5). Hydride complexes (**XV**) have a vacant site for coordination of a new ethylene monomer, giving the corresponding ethylene hydride π-complex

Table 4
Relative energies for the chain propagation step insertion into the imine-nickel(II) **1a**, **2a** and **2a′** systems

System	ΔE_{11}	$\Delta E_{12}^{\#}$	ΔE_{13}
Brookhart **1a**	−14.5	9.3	−3.3
Pyridine **2a**	−12.4	11.1	−2.3
Pyridine **2a′**	−10.1	10.1	−3.5

These energies are expressed in relation to that of the ethylene propyl β-agostic π-complex (**X**). (Energies are given in kcal/mol).

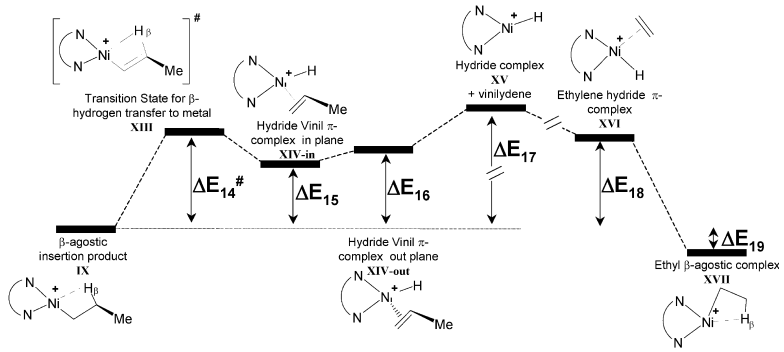

Fig. 5. β-Hydride transfer mechanism for ethylene insertion into the imine-nickel **1a**, **2a** and **2a′** systems. Energies were calculated relative to that of the β-agostic insertion product (**IX**) (values provided in Table 5).

(**XVI**) with a relative energy (ΔE_{18}) of 13.7, 12.2 and 9.7 kcal/mol for the three catalytic systems. Ethylene hydride π-complexes (**XVI**) develop to form the transfer products (**XVII**) which are 1.4, 0.5 and 1.8 kcal/mol lower in energy than the β-agostic insertion product (**IX**). As can be observed, the rate-limiting step for this process is vinyl chain migration, with an activation energy barrier higher than 40 kcal/mol. This process thus appears to be highly unfavourable.

3.4.2. Mechanism of β-hydride transfer to monomer

Energy profiles for the β-hydride transfer to monomer process are shown in Fig. 6 and Table 6. The β-agostic insertion product (**IX**) can coordinate an ethylene monomer to form the ethylene β-agostic π-complex (**X**). The energy of monomer coordination (ΔE_{20}) was 14.5, 13.6 and 13.0 kcal/mol for the **1a**, **2a** and **2a′** catalysts, respectively. β-Agostic interaction in the ethylene β-agostic π-complex (**X**) is considerably weaker than that occurring in the precursor (**IX**) for the **1a**, **2a** and **2a′** systems. Ni–Hβ distances in the **X** complex (2.009, 2.077 and 2.100 Å in **1a**.**X**, **2a**.**X** and **2a′**.**X**, respectively) are much longer than in the precursor **IX** complexes (1.674, 1.664 and 1.670 Å for **1a**.**IX**, **2a**.**IX** and **2a′**.**IX**). The reaction goes through a transition state (**XVIII**) towards a vinyl β-agostic π-complex (**XIX**) by transfer of one hydrogen in β-position from the alkyl chain to the coordinated monomer. The energy barrier ($\Delta E_{21}^{\#}$) associated with this H-β transfer step is 21.7, 21.0 and 17.1 kcal/mol for the **1a**, **2a** and **2a′** systems, respectively (these values calculated as $\Delta E_{20} + \Delta E_{21}^{\#}$ are provided in Fig. 6 and Table 6). The three vinyl β-agostic π-complexes, **1a**.**XIX**, **2a**.**XIX** and **2a′**.**XIX**, show β-agostic interaction (Ni–Hβ distances of 1.942, 2.064 and 2.020 Å, respectively). Finally, the vinyl chain migrates out of the coordination sphere to form the ethyl β-agostic complex (**XVII**), as discussed for the previous mechanism.

In summary, the rate-limiting step during the β-hydride transfer to monomer mechanism is β-hydrogen transfer from the alkyl chain to the coordinated monomer. The energy barrier associated with this process is higher for the Brookhart **1a** than the pyridine **2a** catalyst.

Table 5
Relative energies of β-hydride transfer for the imine-nickel(II) **1a**, **2a** and **2a′** systems

System	$\Delta E_{14}^{\#}$	ΔE_{15}	ΔE_{16}	ΔE_{17}	ΔE_{18}	ΔE_{19}
Brookhart **1a**	13.6	9.9	12.4	48.2	13.7	−1.4
Pyridine **2a**	11.5	10.2	10.7	47.6	12.2	−0.5
Pyridine **2a′**	10.2	8.2	10.5	47.7	9.7	−1.8

These energies are expressed in relation to that of the β-agostic insertion product (**IX**). (Energies given in kcal/mol).

3.4.3. The association mechanism

In this mechanism, the hydride vinyl π-complex (**XIV**) is similar to that formed in the β-hydride elimination process, though the mechanisms differ in terms of migration of the vinyl chain. In the association mechanism, the hydride vinyl π-complex (**XIV**) incorporates an ethylene monomer to form an ethylene–vinyl hydride pentacoordinated π-complex (**XX**). Energy profiles for the association mechanism are shown in Fig. 7 and Table 7. The **XX** complexes were more stable by 0.1, 0.9 and 0.1 kcal/mol for the **1a**, **2a** and **2a′** systems, respectively, than the separate species (vinyl β-agostic π-complex (**XI**) + ethylene). In the ethylene-vinyl hydride pentacoordinated π-complex (**XX**), the ethylene

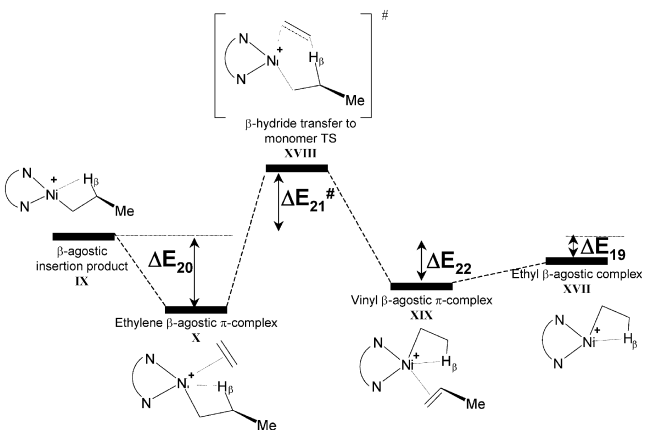

Fig. 6. β-Hydride transfer to monomer mechanism for ethylene insertion into the imine-nickel **1a**, **2a** and **2a′** systems. Energies were calculated relative to that of the β-agostic insertion product (**IX**) (values provided in Table 6).

Table 6
Relative energies of β-hydride transfer to monomer for the imine-nickel(II) **1a**, **2a** and **2a′** systems

System	ΔE_{20}	$\Delta E^{\#}_{21}$	ΔE_{22}	ΔE_{19}
Brookhart **1a**	−14.5	7.2	−4.6	−1.4
Pyridine **2a**	−13.6	7.4	−2.9	−0.5
Pyridine **2a′**	−13.0	4.1	−7.2	−1.8

These energies are expressed in relation to that of the β-agostic insertion product (**IX**).(Energies given in kcal/mol).

Table 7
Relative energies of the association transfer mechanism for the imine-nickel(II) **1a**, **2a** and **2a′** systems

System	$\Delta E^{\#}_{14}$	ΔE_{15}	ΔE_{16}	ΔE_{23}	ΔE_{18}	ΔE_{22}	ΔE_{19}
Brookhart **1a**	13.6	9.9	12.4	−0.1	13.7	−4.6	−1.4
Pyridine **2a**	11.5	10.2	10.7	−0.9	12.2	−2.9	−0.5
Pyridine **2a′**	10.2	8.2	10.5	−0.1	9.7	−7.2	−1.8

These energies are expressed in relation to that of the β-agostic insertion product (**IX**). (Energies given in kcal/mol).

monomer and the vinyl chain are positioned out of plane next to the axial positions. Therefore, the limiting step proposed for this mechanism is β-hydride transfer from the alkyl chain to the metal centre, with energies of 13.6, 11.5 and 10.2 kcal/mol for the **1a**, **2a** and **2a′** systems, respectively.

3.5. Chain transfer reactions vs. propagation step

As seen above, the reaction energies for the propagation step were −3.3, −2.3 and −3.5 kcal/mol for the **1a**, **2a** and **2a′** systems, respectively; while corresponding energies for the chain transfer mechanisms were slightly lower, −1.4, −0.5 and −1.8 kcal/mol for the **1a**, **2a** and **2a′** systems, respectively. Thus, the propagation step is thermodynamically more favourable than the transfer reactions for both catalytic systems.

Similarly, energy barriers for the propagation step are lower than those calculated for the chain transfer mechanism. The β-hydride elimination mechanism is very unlike due to the high energy barrier. Of the two remaining mechanisms, the association one is the most probable. However, it should be pointed out that the β-hydride transfer mechanism to the monomer cannot be ruled out, since the ethylene β-agostic π-complex (**X**) is more stable (ΔE_{20} in Table 6) than the hydride vinyl π-complex (**XIV**-in) involved in the association mechanism (ΔE_{15} in Table 7). In the case of the pyridine complex, both the transfer barriers for the association and the β-hydride transfer to monomer are lower for the **2a′** site.

Table 8 shows that for the Brookhart **1a** catalyst, the difference between the energy barriers corresponding to the propagation step and transfer process was 12.4, for the β-hydride transfer to monomer mechanism, and 4.3 kcal/mol for the association mechanism, while for the pyridine catalyst these values were 10.0 and 7.0 kcal/mol and 0.4 and 0.1 kcal/mol for the **2a** and **2a′** sites, respectively.

Consequently, in line with experimental results [21–23], the molecular weight of the polymer produced using the Brookhart **1a** catalyst will be higher than those yielded by the pyridine catalysts.

4. Conclusions

The different conformations of the cationic active species of Ni(II)-imine based catalysts were observed to greatly influence the ethylene polymerisation process. It seems that the ideal design for these catalysts would include bulky ancillary groups attached to the diimine ligand such that rotation of the aryl ring, which blocks the catalyst's active site, is impaired. The substitution of one of the aryl groups by a pyridine ring makes the chain transfer process easier with respect to the propagation step, giving rise to lower molecular weight polymers in agreement with the experimental results [21–23].

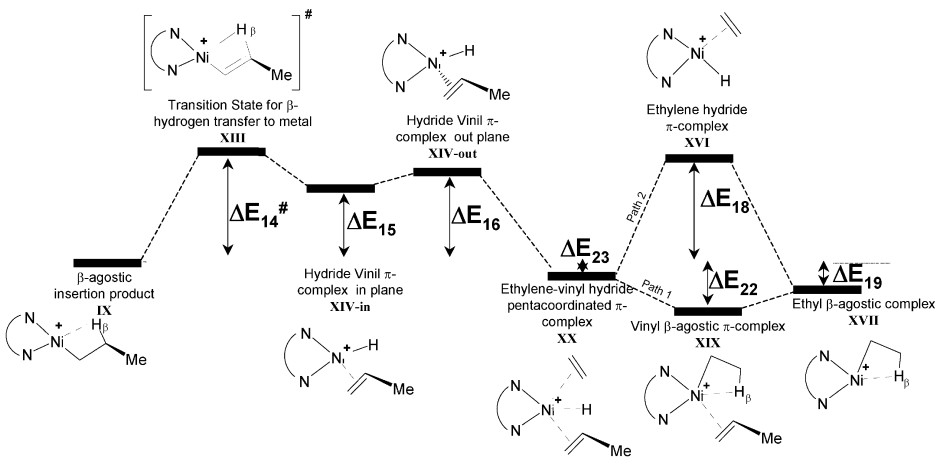

Fig. 7. Association transfer mechanism for ethylene insertion into imine-nickel the **1a**, **2a** and **2a′** systems. Energies were calculated relative to that of the β-agostic insertion product (**IX**) (values provided in Table 7).

Table 8
Energy barrier differences between the propagation and β-hydride transfer to monomer steps

System	β-Transfer to monomer vs. propagation[a]	Association vs. propagation[b]
Brookhart **1a**	12.4	4.3
Pyridine **2a**	10.0	0.4
Pyridine **2a′**	7.0	0.1

[a] Calculated as $(|\Delta E_{20} + \Delta E^{\#}_{21}| - \Delta E^{\#}_{12})$.
[b] Calculated as $(\Delta E^{\#}_{14} - \Delta E^{\#}_{12})$. (Energies given in kcal/mol).

Experimentally, the activities of the Brookhart **1a** and pyridine **2a** catalysts remain unclear [21–23]. Based on the calculated energy barriers for the propagation step and differences in energy barriers for the propagation and chain transfer reactions, the Brookhart **1a** catalyst would be expected to be slightly more active than the pyridine **2a** catalyst.

Acknowledgements

Thanks are due to the MCYT (Grant MAT2002-01242) for funding this investigation. The authors also acknowledge Repsol-YPF, Spain for their permission to publish these data.

References

[1] Soares JBP, Hamielec AE. Polym React Engng 1995;3(2):131–200.
[2] Brintzinger HH, Fischer D, Mülhaupt R, Rieger B, Waymouth RM. Angew Chem Int Ed Engl 1995;34:1143.
[3] Kaminsky W, Sinn H. Transition metals and organometallics for catalysts for olefin polymerisation. New York: Springer; 1988.
[4] Kawamura-Kuribayashi H, Koga N, Morokuma K. J Am Chem Soc 1992;114(19):8687–94.
[5] Meier RJ, Van Doremaele GHJ, Iarlori S, Buda F. J Am Chem Soc 1994;116(16):7274–81.
[6] Yoshida T, Koga N, Morokuma K. Organometallics 1995;14(2):746–58.
[7] Cruz VL, Muñoz-Escalona A, Martínez-Salazar J. Polymer 1996;37(9):1663–7.
[8] Woo TK, Margl PM, Lohrenz JCW, Blöchl PE, Ziegler T. J Am Chem Soc 1996;118(51):13021–30.
[9] Cruz VL, Muñoz-Escalona A, Martínez-Salazar J. J Polym Sci, Part A: Polym Chem 1998;36(7):1157–67.
[10] Muñoz-Escalona A, Ramos J, Cruz VL, Martínez-Salazar J. J Polym Sci, Part A: Polym Chem 2000;38(3):571–82.
[11] Ramos J, Cruz VL, Muñoz-Escalona A, Martínez-Salazar J. Polymer 2000;41(16):6161–9.
[12] Johnson LK, Killian CM, Brookhart M. J Am Chem Soc 1995;117(23):6414–5.
[13] Johnson LK, Mecking S, Brookhart M. J Am Chem Soc 1996;118(1):267–8.
[14] Killian CM, Tempel DJ, Johnson LK, Brookhart M. J Am Chem Soc 1996;118(46):11664–5.
[15] Britovsek GJP, Gibson VC, Kimberley BS, Maddox PJ, McTavish SJ, Solan GA, White AJP, Williams D. J Chem Commun 1998;849.
[16] Britovsek GJP, Bruce M, Gibson VC, Kimberley BS, Maddox PJ, Mastroianni S, McTavish SJ, Redshaw C, Solan GA, Strömberg S, White AJP, Williams DJ. J Am Chem Soc 1999;121(38):8728–40.
[17] Small BL, Brookhart M, Bennett AMA. J Am Chem Soc 1998;120(16):4049–50.
[18] Small BL, Brookhart M. J Am Chem Soc 1998;120(28):7143–4.
[19] Skupinska J. Chem Rev 1991;91(4):613–48.
[20] Ittel SD, Johnson LK, Brookhart M. Chem Rev 2000;100(4):1169–204.
[21] Eilerts NW. Phillips Petroleum Company WO99/49969 Patent; 29 March 1999.
[22] Taine TV, Lappalainen K, Liimatta J, Löfgren B, Leskelä M. Macromol Rapid Commun 1999;20(9):487.
[23] Bres PL, Gibson V, Mabille C, Reed W, Wass D. Weatherhead R BP Chemicals Limited WO98/49208 Patent; 24 April 1998.
[24] Musaev DG, Froese RDJ, Svensson M, Morokuma K. J Am Chem Soc 1997;119(2):367–74.
[25] Strömberg S, Zetterberg K, Sieghbahn PEM. J Chem Soc Dalton Trans 1997;4147.
[26] Deng L, Margl P, Zeigler T. J Am Chem Soc 1997;119(5):1094–100.
[27] Deng L, Woo TK, Cavallo L, Margl PM, Zeigler T. J Am Chem Soc 1997;119(26):6177–86.
[28] Froese RDJ, Musaev DG, Morokuma K. J Am Chem Soc 1998;120(7):1581–7.
[29] Arlman EJ, Cossee P. J Catal 1964;3:99.
[30] Brookhart M, Green MLH. J Organomet Chem 1985;250:395.
[31] te Velde G, Bickelhaupt FM, van Gisbergen SJA, Fonseca Guerra C, Baerends EJ, Snijders JG, Ziegler T. Chemistry with ADF. J Comp Chem 2001;22:931.
[32] Vosko SJ, Wilk L, Nusair M. Can J Phys 1980;58:1200–11.
[33] Perdew JD, Wang Y. Phys Rev B 1986;33:8800.
[34] Becke AD. Phys Rev B 1988;38(6):3098–100.
[35] Ramos J, Cruz V, Muñoz-Escalona A, Martínez-Salazar J. Polymer 2001;42:8019–23.